Tree Physiology 30, 761–772
doi:10.1093/treephys/tpq026

The role of tyloses in crown hydraulic failure of mature walnut trees afflicted by apoplexy disorder

ANDREW J. McELRONE,[1,3] JOSEPH A. GRANT[2] and DANIEL A. KLUEPFEL[1]

[1] *USDA-ARS, Crops Pathology and Genetics Research Unit, Davis, CA 95616, USA*

[2] *University of California, Cooperative Extension, Stockton, CA 95206, USA*

[3] *Corresponding author (ajmcelrone@ucdavis.edu)*

Received November 17, 2009; accepted March 7, 2010; published online May 6, 2010

Summary In the Central Valley of California, mature walnut trees afflicted with apoplexy disorder exhibit rapid and complete crown defoliation within a few weeks of symptom initiation. Symptoms are typically found throughout the entire crown and are initially expressed as wilting and chlorosis followed by scorching of leaves. Since the cause of apoplexy disorder is unknown, we set out to elucidate the water relations physiology underlying this condition. Stem water potential (Ψ_s) of healthy, asymptomatic trees remained high throughout the 2007 growing season, while that of apoplexy-afflicted trees decreased significantly with the onset of symptoms for both healthy-appearing and symptomatic portions of these trees. Ψ_ss were significantly reduced by at least 0.7 MPa in the lower, middle and upper portions of the symptomatic canopies compared with those from asymptomatic trees. Heat pulse velocities measured in the main trunk at three radial depths consistently decreased prior to the onset of symptoms and eventually reached zero with complete crown defoliation. Comparison of sap flow with predicted water use based on walnut evapotranspiration suggests that stomata of symptomatic trees were closing at higher evaporative demand prior to symptom formation. Specific hydraulic conductivity (K_s) of symptomatic stems was significantly lower than that of asymptomatic stems, and no detectable K_s could be measured on several of the symptomatic stem samples. However, shallow root K_s did not significantly differ between symptomatic and asymptomatic trees, suggesting that hydraulic failure was isolated to the crown of these grafted trees. Light and scanning electron microscopy of stem and trunk sapwood revealed extensive tylose development in vessels throughout the crown of symptomatic trees. Analysis of the formation of tyloses on multiple dates revealed rapid development of these vessel occlusions in conjunction with visual symptom formation and dramatic decreases in sap flow. In 2008, tylose development was associated with elevated ethylene production in the active sapwood of symptomatic trees. The cause of elevated ethylene associated with tylose production and symptom formation is yet to be determined.

Keywords: ethylene, Juglans hindsii rootstock, Juglans regia, leaf scorching, sap flow, vascular dysfunction, water relations.

Introduction

Walnuts have been used by humans for over 9 millennia and are now a crop of major economic importance in their primary growing regions (California Walnut Board 2009). California is the world's second largest walnut-growing region and accounts for 99% of the US commercial supply and 66% of the global supply. Demand for walnuts continues to rise in both domestic and international markets, and the commercial production area has risen steadily over the past decade to match consumer demand (Perez and Pollack 2005). In California, there are ~90,000 bearing hectares currently in production with the majority of orchards occurring in the San Joaquin and Sacramento Valleys; these valleys produced over 320,000 tons in each of the past 7 years (Perez and Pollack 2005, NASS 2008, California Walnut Board 2009). The current annual value of this crop is estimated at ~$754 million (NASS 2008). Given the tremendous economic importance of walnut production to both California and the USA, maintaining healthy and productive orchards is critical.

Walnut apoplexy has been described for many decades as a rare disorder of unknown etiology, characterized by sudden midsummer wilting and collapse of mature trees (Ross 1976, Grant et al. 2002). Over the past three decades, the disorder has been documented in orchards in several of California's Central Valley walnut growing districts. During recent multi-year outbreaks, one particularly hard-hit growing area near Clements, CA has lost over 60 ha of mature 30-year-old walnut trees in seven separate orchards.

Leaves of apoplexy-afflicted trees wilt suddenly, turn yellow and then scorched-brown, and abscise from the entire crown within 5–20 days of the onset of symptoms (Ross 1976, Grant et al. 2002). The green outer husks of nuts on symptomatic trees shrivel very rapidly with the onset of leaf symptoms. They later turn black and typically remain attached to the tree.

In most cases, all branches of affected trees die back to the large basal portion of primary scaffolds or to the trunk. Vigorous adventitious shoots often arise later from these parts of the trees (Grant et al. 2002). This combination of symptoms suggests that the disorder is caused by vascular dysfunction associated with vessel occlusion. Leaf scorching, curling and wilting are common symptoms of vascular wilt infections, where xylem conduits become occluded by embolisms, tyloses, gums, bacterial masses and fungal hyphae (Dimond 1955; Newbanks et al. 1983; VanderMolen et al. 1987; Hopkins 1989; Tyree and Zimmermann 2002; McElrone et al. 2008). Similarly, vascular dysfunction has been associated with rapid tylose formation due to nonpathogenic wounding and elevated ethylene (Pérez-Donoso et al. 2006; Sun et al. 2008). Alternatively, English walnut (*Juglans regia* L.) is known to rapidly develop chlorosis and drop its leaves under drought conditions (Tyree et al. 1993). Any one or a combination of these factors may be involved in walnut apoplexy disorder.

Walnut apoplexy occurs most commonly in older orchards planted on coarse to medium textured sandy loam soils (Ross 1976, Grant et al. 2002). The disorder is more common in orchards established on Northern California black walnut (*Juglans hindsii* (Jeps.) Jeps. ex R.E. Sm.) than in orchards on 'Paradox' hybrid (*J. hindsii* × *J. regia* L.) or other rootstocks, but this may be due to the prevalence of black walnut rootstocks in older orchards. However, there is no evidence that scion cultivars differ in susceptibility to apoplexy. Empirical and experimental attempts to link walnut apoplexy to known biotic causes, soil moisture status, nutrient applications, deficiencies and toxicities have been unsuccessful or inconclusive (Grant et al. 2002).

Despite the historical documentation of apoplexy disorder, to our knowledge no research has been conducted to understand how this disorder affects the vascular structure and function of afflicted trees. Given the recent emergence of apoplexy in some regions, work is needed to address this research gap since growers are faced with the choice of continually replanting or complete removal of their afflicted orchards. In this study, we elucidate the physiological mechanism involved in rapid crown collapse using a variety of plant water relations and anatomical assessments on symptomatic and healthy, asymptomatic trees in a mature walnut orchard with a history of apoplexy. Since apoplexy symptoms resemble an unusually rapid onset of drought-induced leaf chlorosis and drop that is known for English walnut (*J. regia* L.) (Tyree et al. 1993), we used a variety of water relations and anatomical analyses to address the following hypothesis: walnut apoplexy is caused by hydraulic failure associated with vessel occlusion by embolism or tylose formation.

Methods

Site and tree descriptions

This study was conducted at the Biglieri ranch, a mature 30-year-old walnut orchard located near Lockeford, CA (38° 11.505′ N, 121°06.145 W). This site (and adjoining orchards) had a history of serious recurring apoplexy problems resulting in the loss of large sections of the orchard prior to and during the study period. *J. regia* cv. Tehama scion grafted onto *J. hindsii* rootstock were planted in 1968 on 9.14 m spacing between rows and between trees in a row. The mean scion trunk diameter of all the study trees ranged from 31.2 to 42.8 cm with a mean of 36.0 cm at ~1.5 m above the ground surface. The orchard is located in the Mokelumne River flood plain, and the soils are deep, dark and well drained. Since the late 1970s, the orchard has been impact sprinkler-irrigated at 2- to 4-week intervals to replace water losses due to evapotranspiration.

At the beginning of the 2007 growing season, five trees were assigned to an asymptomatic group (i.e., expected to remain healthy/symptomless), and five trees were assigned to a symptomatic group (i.e., expected to exhibit symptoms). These groupings were made based on the trees' proximity to the advancing front of apoplexy symptoms tracked by the orchard owner during the 2006 field season. The original asymptomatic group was located four rows back into the orchard in an attempt to ensure that they remained symptomless. However, only one of these trees remained asymptomatic throughout the entire study, and additional asymptomatic trees were designated as needed. Sap flow sensors were installed in all 10 trees in early May 2007, and Ψ_s measurements commenced on all trees at this same time and continued throughout the season.

In early June 2007, another set of trees, which were separated by four trees from the original symptomatic group, were the first in the orchard to exhibit symptoms. Sap flow sensors were immediately installed on six of these newly symptomatic trees. In total, we tracked sap flow and Ψ_s measurements on 15 symptomatic trees.

Stem water potentials (Ψ_s)

Midday stem water potentials (Ψ_s) were measured on approximately a weekly basis throughout the 2007 growing season using a pump-up Scholander-type pressure chamber (PMS Instruments, Albany, OR) for all measurements. Fully expanded terminal leaflets were selected randomly at a consistent height 3–4 m from the ground and were enclosed in foil-laminate bags (PMS Instruments) for at least 15 min prior to measurements. In this growing region, bagged leaf Ψ are used commonly in walnut orchard management as a proxy of Ψ_s to track tree water status for irrigation scheduling. During one sampling on 29 June, more intensive measurements were performed at additional crown locations (i.e., lower, middle and upper at ~3, 6 and 9 m, respectively) to: (i) assess spatial variations in Ψ_s and their relation to visual apoplexy symptoms and (ii) compare healthy-appearing and symptomatic portions of symptomatic trees. Given the large height of these mature trees, a mobile aerial lift was used to access leaves in the upper portions of tree canopies. On each sampling date, at least four subsamples were taken from each height within each of four symptomatic and asymptomatic trees.

Sap flow and microclimatic measurements

Sap flow was measured in the main trunk of the walnut trees using the heat ratio method (HRM) developed by Burgess et al. (2001) and with sensors designed by East 30 Sensors, Inc. (Pullman, WA). Two temperature sensor needles containing type-E thermocouples were installed symmetrically and in parallel in sapwood at 6 mm distance above and below a line heater needle containing a coiled heating element (~42 Ω). Each temperature sensing needle contained three thermocouple junctions spaced 12.5 mm apart in order to measure radial patterns of flow at 5.0, 17.5 and 30.0 mm depth into the sapwood. Any potential spacing errors between the thermocouple and heater needles were minimized by using a drill guide. A short pulse of heat was released into the sapwood, and the resultant heat pulse velocity was calculated according to Burgess et al. (2001) using the following equation: $V_h = (k/x) \times \ln(v_1/v_2) \times 3600$, where k is the thermal diffusivity of fresh wood, x is the distance (cm) between the heater and either temperature probe, and v_1 and v_2 are the increases in temperature after the heat pulse at equidistant points downstream and upstream, respectively, at x cm from the heater. We used established protocols outlined in Burgess et al. (2001) to correct data for errors caused by incorrect probe spacing/alignment and wounding around drill holes. Sapwood properties (basic density of the wood and water content of the sapwood) were determined using increment cores extracted from all study trees.

Microclimatic data were recorded at a weather station located in an open field adjacent to the study orchard for comparison with sap flow and other physiological measurements. Air temperature and relative humidity were measured using a HMP45C probe (Campbell Scientific, Logan, UT) and recorded with the same data logger (CR10X; Campbell Scientific) used for sap flow measurements.

In order to determine stomatal responses prior to the onset of symptoms, we compared our sap flow measurements with predicted evapotranspiration for walnuts calculated using a California Irrigation Management Information System (CIMIS) monitoring station located in close proximity to our field site. Midday mean heat pulse velocities were calculated using the 10 AM to 2 PM values for each day for each of the symptomatic trees represented in Fig. 3. CIMIS uses a well-watered actively growing closely clipped grass that is completely shading the soil as a reference crop to calculate reference evapotranspiration (ET_o) at this monitoring station. A crop coefficient (K_c) specific to mature walnuts growing in this region was used to calculate actual evapotranspiration (ETc) using the following equation: $ETc = ET_o \times K_c$. A comparison of microclimatic data collected at our field site with that of the nearest CIMIS station revealed a strong linear relationship between weather parameters measured at both sites (linear regression comparing $VPD_{CIMIS} = 0.88 \times VPD_{field\ site} + 2.57$, $R^2 = 0.82$). Additional details about CIMIS can be found at www.cimis.water.ca.gov.

Specific hydraulic conductivity and embolism of stems and roots

We followed the methods of Sperry et al. (1988) to measure specific hydraulic conductivity (K_s) and native embolism on stems and shallow roots from asymptomatic and symptomatic trees. Stem and root segments were collected from trees, wrapped in humidified plastic bags and transported immediately to the lab for measurements. Shallow roots were excavated from the soil, using hand trowels, traced back to the trunks to ensure connectedness to each study tree and excised. In the lab, segments were recut underwater, shaved at the ends with razor blades, and attached to a tubing manifold filled with filtered, degassed, deionized water. Segment lengths were larger than the longest vessel for each organ, and diameters for both stem and root segments were limited to a specific size range (~8–15 mm) to control for size and age effects. Hydraulic conductance (K_h) was then measured as the quotient of the mass flow rate of solution through the segment and the pressure used to drive the flow. A Mariotte bottle was used to deliver a constant head pressure of 10 kPa, and mass flow was measured continuously at 10 s intervals and calculated from a running mean of five sequential readings. K_s was calculated as: $(K_h/A) \times L$, where A is the cross-sectional area of the xylem without bark and cortex and L is the segment length. Native embolism was determined by flushing the segments with the perfusing solution at high pressure (~100 kPa) for 30 min and re-measuring maximum K_s after air bubbles were removed. Native embolism was then calculated using the equation: $1 - (K_s \text{ initial}/K_s \text{ maximum}) \times 100$. This method has been used successfully in previous studies to distinguish embolism and vessel occlusion associated with vascular dysfunction in other tree species (e.g., McElrone et al. 2003, 2008).

Microscopy for quantification of tylose incidence

Stem samples were cut into 30-µm-thick sections with a sliding microtome (Leica SM 2000R, Leica Microsystems, Bannockburn, IL). Sections were then dehydrated and cleared in an ethanol–xylene series incorporating a 4-h staining with 1% safranin O at the 50% ethanol step and a 1-min staining with 0.5% fast green FCF at the 95% ethanol step (Ruzin 1999). Prior to visualization of the cross-sections with a light microscope, the samples were rehydrated to water with the same ethanol–xylene series, and mounted with a coverslip in glycerol. Sections were observed at ×100 to ×400 with a compound light microscope equipped with a digital camera (Leica DFC295; Leica Microsystems). Additional stem samples from both asymptomatic and symptomatic trees were viewed using a Philips XL 30 Environmental Scanning Electron Microscope (ESEM; FEI Company, Eindhoven, The Netherlands) in the Biological Sciences SEM Facility at Duke University in Durham, NC to verify the presence of tyloses.

After determining that tyloses were present in vessels of symptomatic stem samples, we quantified the number of

vessels containing tyloses and the extent of occlusion (by focusing up and down through a cross-section) in replicated stem samples for both asymptomatic and symptomatic trees. For each sample, several sectors within each cross section containing numerous vessels were chosen randomly for analysis. All vessels in each sector were categorized as: vessels without tyloses, partially filled with tyloses or completely occluded with tyloses. Samples used in this analysis were collected from several stems ($n \geq 5$) for both asymptomatic and symptomatic trees. In late August 2007, we also collected 60-mm deep increment cores from the trunks of trees ~1.5 m above the ground to determine the extent of tylose development in trunk sapwood. Cores were collected from $n \geq 5$ replicate trees in each crown category. These cores were divided into three radial depth categories: 0–20 mm (outermost annual rings), 20–40 mm and 40–60 mm (innermost annual rings closest to the heartwood). Cross-sections of the cores were prepared with a sliding microtome, and all vessels in each radial depth were analyzed for the presence and extent of vessel occlusion as described above for stem samples.

Ethylene sampling

During the 2008 growing season, we measured ethylene concentrations in the trunks of asymptomatic and symptomatic trees using methods described by Eklund (1990, 2000). Once symptoms began developing in late July, we identified several symptomatic and asymptomatic trees ($n \geq 5$ for each category) to be used in the ethylene sampling. On the trunk of each tree at a height of ~1.5 m above the ground, 10 mm diameter holes were drilled through the bark and to a position 10 mm inside the cambium. Acid-resistant stainless steel tubes were inserted into the holes and sealed in position with silicone caulking to prevent leakage. A gas-tight rubber stopper was inserted into the end of each steel tube. A glass vial sealed with a gas-tight rubber stopper was connected to the rubber stopper on the steel tube through a double-ended needle. The double-ended needle connected the air in the steel tube to that in the glass vial and allowed gases to equilibrate within the tube–vial setup. At each sampling date, the glass vials were collected and replaced immediately with new vials. The ethylene concentrations in the samples were determined with an analytical gas chromatograph (Carle Instruments) fitted with a photoionization detector (model PI-51-01; HNU Systems) using the standard protocols of the Post Harvest Research and Information Facility at the University of California, Davis.

Statistical analysis

Statistical analysis of Ψ_s, K_s, native embolism, tylose and ethylene data was performed using a univariate general linear model (GLM) program in SAS 9.1 (SAS Institute Inc., Cary, NC). Least squares (LS) Means were used to distinguish between individual treatments when needed.

Results

Symptom description and seasonal development

Numerous trees within the study orchard developed symptoms throughout the summer of 2007, including trees located on the orchard edge of where trees had succumbed to the disorder in 2006. In 2007, symptoms first appeared on several trees in the orchard on 1 June, and additional trees developed symptoms on 4, 15 and 28 June; on 6, 13 and 18 July; and on 1 and 14 August. Trees in the study orchard exhibited typical apoplexy symptoms (Fig. 1) as described previously (Grant et al. 2002). Symptoms were initially expressed as sudden wilting, chlorosis and scorching of leaflets, initially detected on single branches and leaves, but quickly spread to the entirety of symptomatic canopies (Fig. 1). Once leaves exhibited initial symptoms, the entire crown was typically defoliated within a few weeks (Fig. 1A). Several weeks to months after defoliation, symptomatic trees exhibited adventitious shoot re-growth from the trunk and large main branches (Fig. 1D). These re-sprouts would often exhibit symptoms and defoliate shortly after emergence.

Counter to suggestions by other researchers (Ross 1976), we found no clear linkages between symptom onset for individual trees and the climate patterns or timing of irrigation events. For example, a large group of trees first showed symptoms in early June when air temperatures were mild and vapor pressure deficit (VPD) was low, while others developed symptoms on 6 July when air temperatures and VPD approached the seasonal maximums.

Stem water potential (Ψ_s)

Ψ_s were consistently lower throughout the entire crown of symptomatic trees compared with similar heights ($P < 0.0001$; Fig. 2) and compass directions (data not shown) in asymptomatic trees. Symptoms were distributed evenly throughout the entire crown based on both visual inspections and Ψ_s measurements. Ψ_s of healthy-appearing stems (i.e., green) on symptomatic trees were also reduced significantly compared with those on asymptomatic trees ($P < 0.0001$) but to a lesser extent than symptomatic stems (i.e., yellow) on symptomatic trees (Fig. 2).

Ψ_s were similar between asymptomatic and symptomatic trees early in the season but diverged with the onset of symptoms. Asymptomatic trees exhibited Ψ_s between −0.45 and −1.0 MPa consistently throughout the season and never approached −1.3 to −1.7 MPa, which is considered a severe water stress threshold for irrigation management in walnuts (see http://ucmanagedrought.ucdavis.edu/walnuts.cfm). Similarly, symptomatic trees exhibited Ψ_s between −0.5 and −1.2 MPa prior to symptom onset early in the growing season (Fig. 3), matching patterns measured in asymptomatic trees. For some symptomatic trees (see Trees 0 and 8; Fig. 3), Ψ_s began to drop around the first appearance of symptoms and continued to decrease as symptoms spread

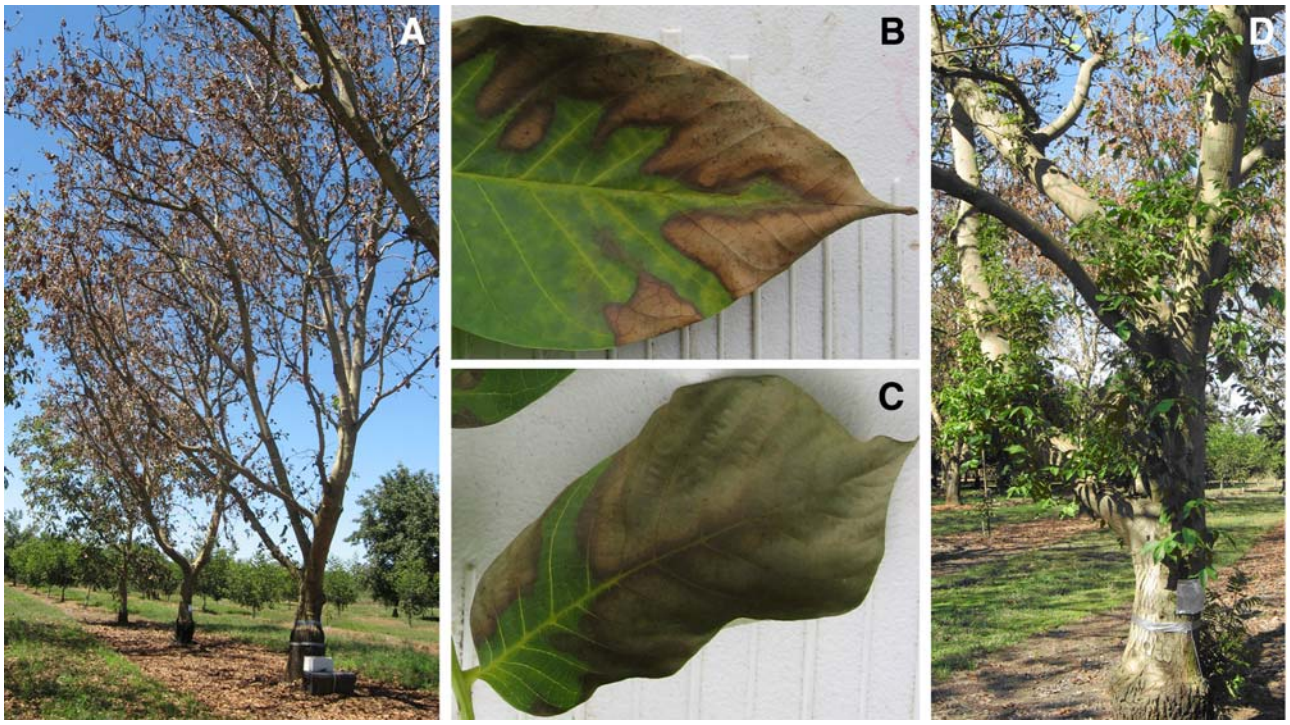

Figure 1. Visual symptoms of walnut apoplexy in aerial parts of symptomatic trees. Symptoms are found throughout the entirety of the crown (A), are initially expressed as scorching and chlorosis at the edge of leaflets (B and C) and culminate in curling of the leaflets and ultimately leaf drop. Once leaves on a given tree start to show scorching symptoms, the entire crown is usually defoliated within a few weeks. Several weeks to months after initial crown defoliation, symptomatic trees will often exhibit adventitious shoot re-growth from the trunk and main branches (D). The re-growth would then scorch and defoliate shortly after reemergence.

throughout the entire crown. However, other trees exhibited decreases in Ψ_s prior to the onset of symptoms (Trees 1, 4 and 5 in Fig. 3).

Sap flow measurements

Patterns of heat pulse velocity were similar at each radial depth (i.e., outer, middle and inner) for asymptomatic and symptomatic trees prior to the onset of symptoms early in the growing season. For all symptomatic trees, sap flow velocity decreased prior to the onset of visual symptoms (Fig. 3). In contrast to the seasonal Ψ_s measurements, sap flow velocity always decreased prior to the onset of visual symptoms for symptomatic trees (Fig. 3, all panels); this pattern is particularly clear for the middle and outer radial depths. Decreased water transport prior to symptom onset was confirmed by comparing midday rates of sap flow with the predicted evapotranspiration for walnuts in this growing region (Fig. 4). In the 2 weeks prior to symptom formation, midday sap flow rates decreased significantly relative to water use patterns predicted from the evaporative demand during this time ($P < 0.0001$; Fig. 4).

Once symptom expression expanded to the entire crown, sap flow activity ceased completely in the outer and middle depths after leaf drop. However, sap flow reactivated only in the oldest xylem (see Fig. 5, bottom panel at about 1 September) upon adventitious re-growth (Fig. 5, bottom panel) but then dropped again in mid-September. This pattern suggests that the re-growth shoots were hydraulically linked to the older xylem at greater radial depth. Some symptomatic trees exhibited increases in nighttime sap flow with the onset of symptoms as seen by constant flow velocities ≥ 6 cm h^{-1} in late June and early July (Fig. 5). A similar pattern was documented at the innermost depth only when the adventi-

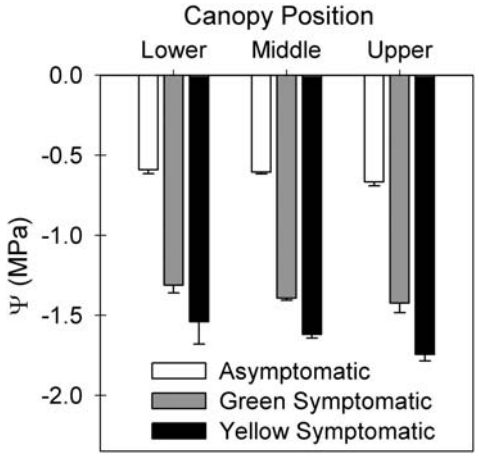

Figure 2. Midday stem water potentials (Ψ) measured on symptomatic and asymptomatic walnut trees on 29 June 2007. Asymptomatic leaves were sampled from trees without symptoms. Shortly after symptoms first appeared in symptomatic trees, green and yellow symptomatic leaves were sampled from healthy-appearing and symptomatic portions of symptomatic trees, respectively. Data represent the mean ± SE for $n \geq 4$ for each sampling category.

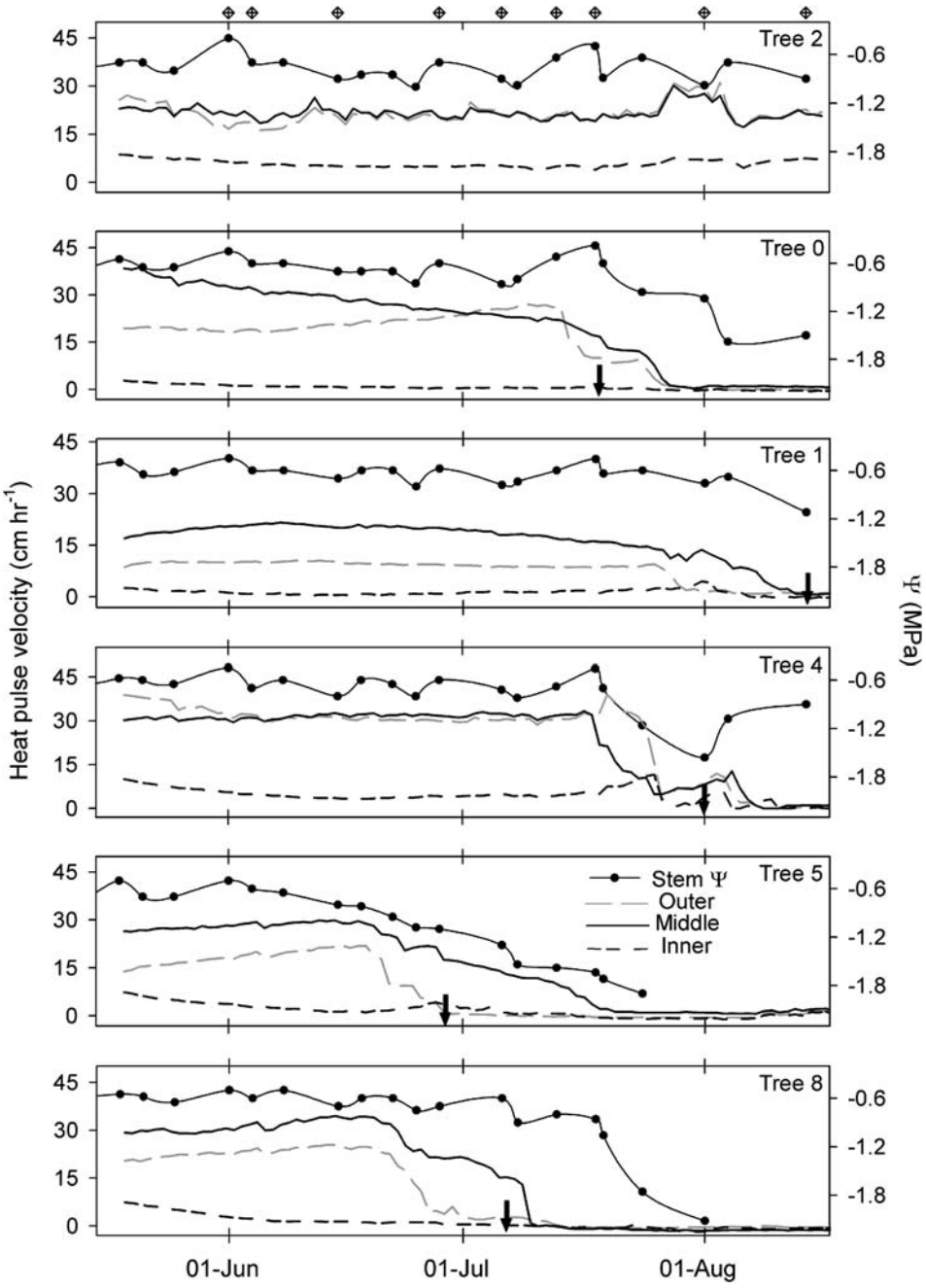

Figure 3. Examples of the seasonal progression of midday stem water potential (Ψ) and midday (10 AM–2 PM) mean heat pulse velocity measured on one asymptomatic (Tree 2, top panel) and five symptomatic (Trees 0, 1, 4, 5 and 8) walnut trees in the 2007 growing season. The numbering on the trees represented here is consistent with that used in Figure 8 for comparison. Black solid arrows at the bottom of each panel represent the date when visual symptoms were first detected for each symptomatic tree. Diamonds across the top of the upper panel represent the dates when irrigation was applied within the walnut orchard.

tious re-sprouts began to show symptoms in mid-September (Fig. 5, bottom panel).

Stem and root specific hydraulic conductivities (K_s) and native embolism

K_s differed significantly between symptomatic and asymptomatic trees, but these differences were limited to the aerial portions of the plants (Fig. 6). These measurements were taken in early June in conjunction with the Ψ_s measurements represented in Figure 2. Stem K_s was significantly lower in symptomatic and asymptomatic stems of symptomatic trees compared with asymptomatic stems from healthy, asymptomatic trees ($P < 0.0001$; Fig. 6). In several of the samples from symptomatic trees, stem K_s reached zero as no fluid could be passed through these samples. Interestingly, K_s was signif-

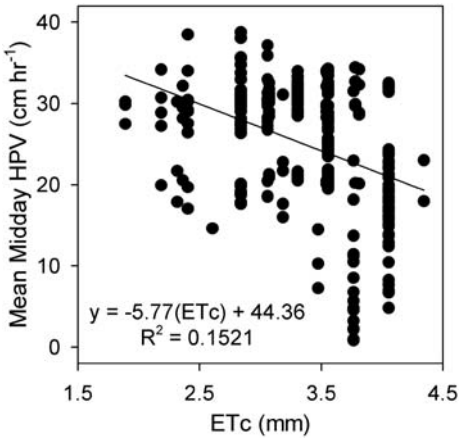

Figure 4. Mean midday heat pulse velocities (HPV) measured on symptomatic trees for ~15 days just prior to symptom initiation measured across a range of crop evapotranspiration calculations (ETc) estimated for mature walnut trees growing in this region. ETc was calculated using data from a nearby California Irrigation Management Information System station and a crop coefficient specific to mature walnuts grown in this region. The equation for the asymptomatic response curve for this same relationship is: $y = 0.97(ETc) + 20.71$, $R^2 = 0.1698$.

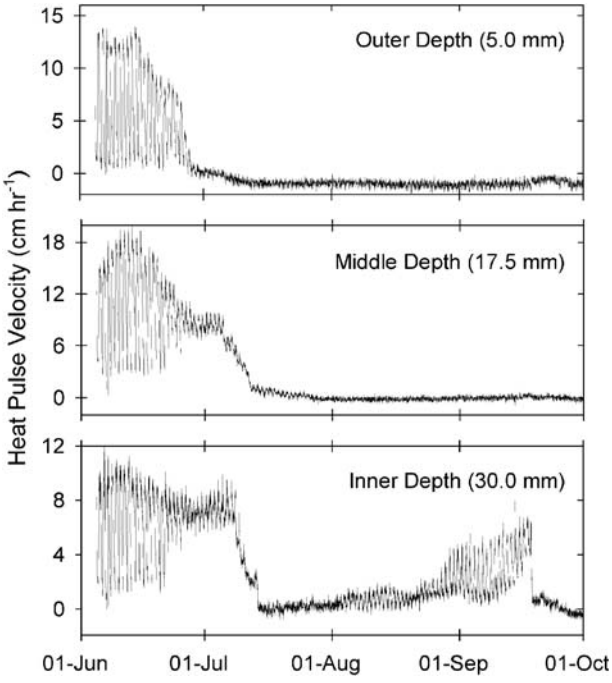

Figure 5. Heat pulse velocity measured at three radial depths in a symptomatic walnut tree. Visual symptoms were first detected in this tree on 1 June. Sensors were installed in this tree in the days immediately following symptom detection. Note the continuous flow detected throughout the day in early July.

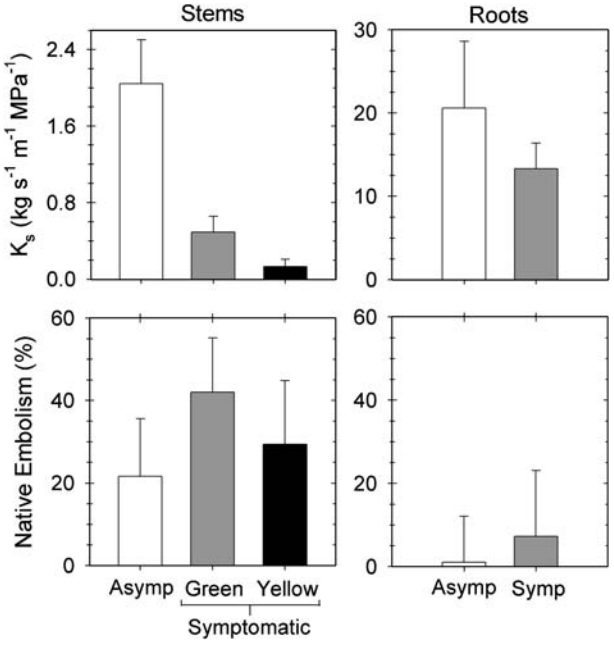

Figure 6. Specific hydraulic conductivity (top panels) and native embolism (bottom panels) measured on stems (left column) and shallow roots (right column) of asymptomatic (Asymp) and symptomatic walnut trees in early June 2007. Similar to the stem Ψ sampling scheme represented in Figure 2, stems were sampled from asymptomatic trees and from healthy-appearing (green) and symptomatic (yellow) branches of symptomatic trees. Shallow roots were collected from asymptomatic and symptomatic (Symp) trees at the field site. Note the difference in axes between the hydraulic conductivity panels between stems and roots. Data represent the mean ± SE for each of $n \geq 5$ replicate samples for each sampling category.

icantly reduced in asymptomatic stems from symptomatic trees but to a lesser degree than the symptomatic stems. This pattern is consistent with that seen in Ψ_s measurements (see green symptomatic in Fig. 2) and suggests that hydraulic failure was slightly more advanced in the symptomatic branches of symptomatic trees but was progressing very rapidly in healthy-appearing portions of symptomatic trees.

A second round of stem K_s measurements, performed on newly symptomatic and healthy trees in late August, demonstrated that stems from healthy, asymptomatic trees maintained similar K_s values throughout the growing season; mean stem K_s of asymptomatic trees in late August measured 2.55 (0.43 SE) kg s^{-1} m^{-1} MPa^{-1}. Stem K_s for the newly symptomatic trees was reduced to 0.08 (0.06 SE) kg s^{-1} m^{-1} MPa^{-1}similar to those from early June.

Root K_s was significantly greater overall than stem K_s ($P < 0.0001$) but was not significantly affected by the presence of symptoms in the crown ($P > 0.05$; Fig. 6, upper right panel). Overall, native embolism was greater in stems than in roots, but crown conditions had no significant effect on this parameter in either organ ($P > 0.265$ for both root and stem native embolism; Fig. 6, bottom panels). In total, the hydraulic measurements suggest a physical blockage isolated to the stems not directly related to reversible embolism.

Quantification of tyloses

Wood anatomical assessments revealed xylem vessels of symptomatic trees blocked with extensive tyloses (Figs.

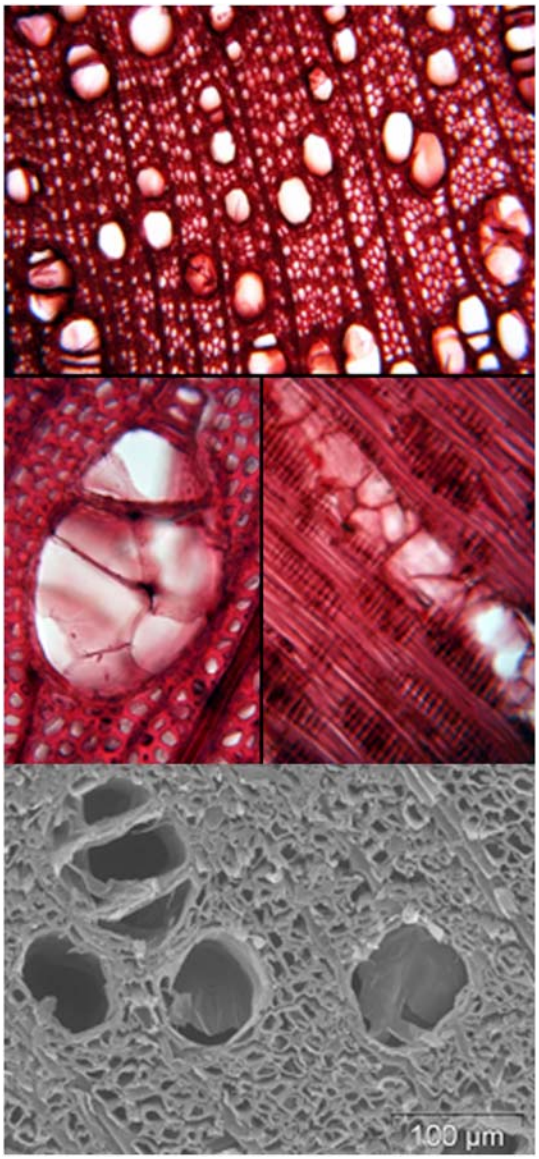

Figure 7. Evidence of tyloses from light microscopy (top three images) and environmental scanning electron microscopy (bottom image) in stem xylem vessels from symptomatic walnut trees. Numerous vessels containing tyloses can be seen in the cross-section at low (top panel) and high (middle panels) magnification. All sections represent xylem from the most recent annual ring. Similar cross-sectional images were used to quantify the percentage of vessel occlusion for the data represented in Figures 8 and 9.

7, 8 and 9). Images from both light and scanning electron microscopy revealed the extent of blockage across a segment (i.e., in many vessels of a cross section) as well as within a single vessel (i.e., lumen entirely blocked) (Fig. 7, middle and bottom panels). Quantification of the extent of tylose development verified that symptomatic stems contained greater numbers of partially and fully blocked vessels than stems of asymptomatic trees ($P < 0.0001$). Trees that became symptomatic between stem sampling dates all showed a significant increase in the quantity and/or severity of tylose blockage (Fig. 8). For example, symptoms were first detected in Trees 1 and 4 on the 14th and 1st of August, respectively, and tylose formation increased dramatically from the sampling on 9 July to that on 29 August (Figs. 3 and 8). This period of rapid tylose formation corresponds with sap flow plummeting to zero for all five symptomatic trees (Figs. 3 and 8). Asymptomatic trees showed little to no tylose development in stem samples analyzed at different points throughout the season (Tree #2 on different sampling dates; Fig. 8). The trend for Tree #2 is representative of a larger group of trees that remained asymptomatic throughout the study and always had <5% of vessels exhibiting tyloses on any date.

Analysis of increment cores extracted from trees of both conditions revealed consistent tylose development throughout the radial profile of symptomatic tree trunks (Fig. 9). In other words, xylem of all ages (i.e., depths) in the trunks was equally susceptible to tylose formation. Conversely, asymptomatic trees exhibited no tyloses in xylem of the most recent annual rings (0–20 mm depth) and only ~20% blockage (partial + full blockage combined) in older xylem (20–60 mm depth), which is typical of xylem transitioning to heartwood formation (Fig. 9). Tree core data combined with stem sampling (Fig. 8) illustrate that the response is found in all wood of the crown (i.e., both stems and trunks showed increased tylose development).

Ethylene sampling

In the summer of 2008, ethylene production was measured in the trunks of asymptomatic and symptomatic trees. Ethylene production was consistently greater across all sampling dates in the symptomatic trees compared with asymptomatic trees (repeated measures ANOVA, $P < 0.05$; Fig. 10).

Discussion

The work presented here sheds light on the physiological mechanisms associated with apoplexy symptom development in walnuts and provides insight into possible solutions for this devastating disorder. Our results indicate that walnut apoplexy disorder results from hydraulic dysfunction induced by rapid tylose formation and irreversible occlusion of sapwood vessels in afflicted trees. Tyloses were detected throughout all parts of symptomatic canopies including petioles, stems and several depths in trunk sapwood. As the tyloses rapidly occlude vessels throughout the tree, the K_s of crown organs decreases and induces stomatal closure and reduced sap flow prior to symptom onset. Increases in the hydraulic resistance of walnuts are known to induce stomatal closure and maintain leaf Ψ above a cavitation-inducing threshold (Cochard et al. 2002). Elevated ethylene levels, which have been recently implicated in rapid tylose formation (Sun et al. 2007; see details below), were detected in the sapwood of symptomatic trees, but the cause of the elevated ethylene is currently unknown.

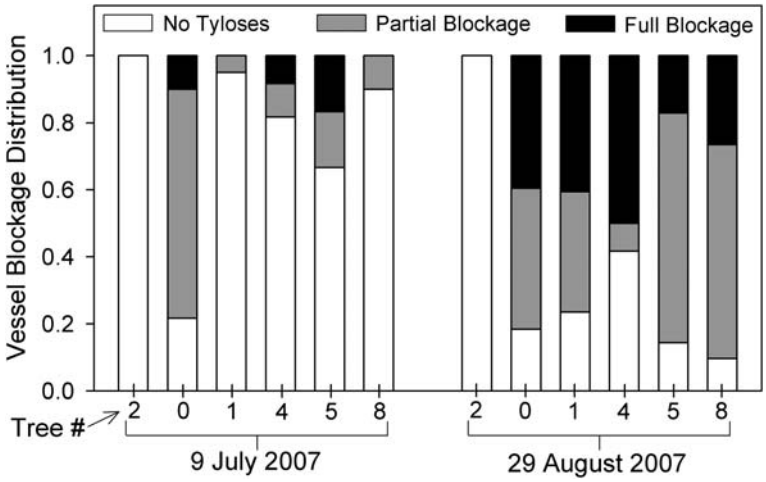

Figure 8. Changes in vessel status over time for stems sampled from an asymptomatic tree (# 2) and five symptomatic trees (# 0, 1, 4, 5 and 8). Visual symptoms were detected in each of the symptomatic trees between 28 June and 14 August 2007 (see Fig. 3 for specific dates of symptom onset for these same trees). Stem samples were collected from each tree on each of the sampling dates, and the data represent a mean of three subsamples from three replicate stems for each tree on each date. Data from these trees represent the general pattern seen among all trees in each of the crown categories. Tree # 2 is an example of an asymptomatic tree that remained as such throughout the entirety of the 2007 and 2008 growing seasons.

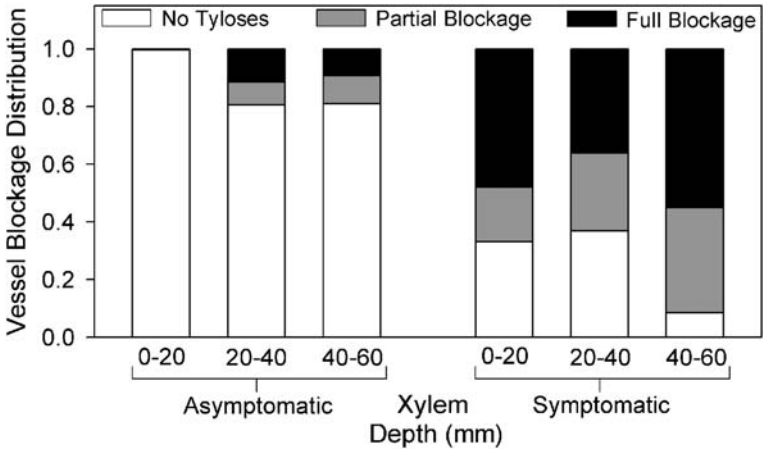

Figure 9. Tylose distribution based on depth into trunk wood for healthy, asymptomatic and symptomatic walnut trees. Cores were collected in late August 2007 at ~1.5 m height using an increment corer from at least five trees in each crown category. The 0–20 mm depth represents the xylem from the most recent annual rings. Data represent means from $n \geq 5$ replicate cores for each symptomatic crown category.

Tyloses are outgrowths of parenchyma cells that emerge through vessel-parenchyma pits into vessel lumen and are common in a wide range of tree species (Esau 1977, Bonsen and Kučera 1990, Tyree and Zimmermann 2002). Tyloses contain a suberized wall layer, which impedes fluid penetration (Parameswaran et al. 1985) and reduces or eliminates the hydraulic conductivity of an occluded vessel (Dimond 1955, Aleemullah and Walsh 1996, Parke et al. 2007; Collins et al. 2009). Given the extent of tylose occlusion, it was clear why stems from symptomatic trees exhibited low or negligible stem K_s. For most species, tylose formation is a natural part of xylem aging (Ranjani and Krishnamurthy 1988) and leaf senescence (Dute et al. 1999). However, it can also be triggered by abiotic and biotic stresses such as flooding (Davison and Tay 1985), freezing (Cochard and Tyree 1990), mechanical wounding (Sun et al. 2006) and pathogen infection (Dimond 1955).

Plant biosynthesis of ethylene, a gaseous phytohormone, occurs in response to many of the same biotic and abiotic factors that induce tylose formation (Abeles et al. 1992, Taylor et al. 2002). Sun et al. (2006, 2007, 2008) provided compelling evidence for the link between ethylene production and tylose formation in pruned grapevines. They treated grapevine stems with aminoethoxyvinylglycine (an inhibitor of ethylene biosynthesis) and silver thiosulfate (an inhibitor of ethylene action), both of which delayed and greatly reduced the size and number of tyloses formed after pruning (Sun et al. 2007). Similarly, van Doorn et al. (1991) found that eth-

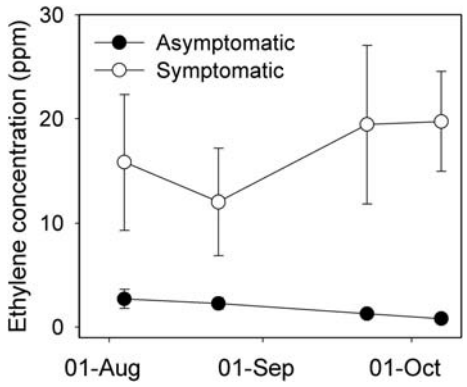

Figure 10. Changes in ethylene concentration sampled in situ from xylem of asymptomatic and symptomatic walnut trees during the 2008 growing season. Data represent the mean ± SE of $n \geq 5$ replicate samples at each sampling point.

ylene synthesis inhibitors suppressed tylose formation and maintained xylem hydraulic conductance, which delayed time to wilting in cut flowering stems of lilac. Ethylene production in symptomatic trees was greater than four times the levels recorded in asymptomatic trees. We hypothesize that elevated ethylene levels induced tylose formation leading to apoplexy symptoms in the walnut trees. However, this hypothesis requires further investigation to determine whether spikes in ethylene production precede tylose formation.

Abiotic factors may be responsible for the increased ethylene production and resulting tylose formation measured in apoplectic walnut trees. Flooding has been found to increase ethylene production in aboveground portions of plants (Hunt et al. 1981, Voesenek et al. 1990) and was also associated with an increase in xylem vessel tylosis (Davison and Tay 1985). Kallestad et al. (2007) found that flood irrigation, in combination with high temperatures, induced marginal leaf necrosis and shuck dieback in pecan and suggested that stress-induced early senescence in these trees was due to elevated ethylene or root damage. Over-irrigation is known to cause significant problems such as leaf drop, decreased yields and crown decline/dieback in California walnut orchards (Lampinen et al. 2004). In both years of our study, there were several times in the early spring and summer when water pooled on the soil surface for >24 h following an irrigation event. Ross (1976) suggested that walnut apoplexy symptoms often appeared shortly after an irrigation event, which may kill the smallest roots in a short period of time, thereby disrupting the tree's ability to absorb water. Even though midday Ψ_s fell within the range of well-watered to mild water stress (Fulton et al. 2002, Lampinen et al. 2004), repeated water pooling events may have caused a cumulative hypoxic stress effect on these mature trees or altered ethylene production in the root zone as documented previously (Hunt et al. 1981, Arshad and Frankenberger 1991). However, flood irrigation, which is still used in many California orchards, does not seem to result in widespread apoplexy, so other site-specific factors may be involved in symptom development.

Tyloses developed over a very short period of time throughout the entire crown of symptomatic trees. Previous studies have shown that tyloses can develop very quickly in response to stress. For example, tyloses develop in grapevine stems as quickly as 1 day after pruning and are found in ~85% of vessels after only 6 days (Sun et al. 2006). Tyloses have also been observed as early as 1–3 days after pathogen inoculation in vascular wilt pathosystems (e.g., VanderMolen et al. 1987, Jacobi and MacDonald 1980). We observed rapid and uniform development of tyloses in walnut canopies resulting in complete crown defoliation ~2–3 weeks after initial symptom detection. Sap flow also plummeted dramatically, suggesting rapid reduction in stem K_s. No significant reduction in root K_s was found in symptomatic trees relative to asymptomatics. This suggests that ethylene was either only produced in the *J. regia* scion or produced throughout the whole tree with *J. hindsii* rootstock being unaffected. However, there was a trend for lower root K_s in symptomatic trees (Fig. 6), suggesting that tylose formation in roots was delayed relative to the aboveground parts.

Ethylene and tyloses are known to play a role in heartwood formation in many tree species (Shain and Hillis 1973, Nelson 1978, Taylor et al. 2002). Tyloses commonly form as sapwood transitions to heartwood (Parameswaran et al. 1985), but their formation in deciduous trees is usually limited to dormant periods when cambial and vascular activity is low (e.g., Cochard and Tyree 1990). In black walnuts, peak ethylene production coincides with the onset of heartwood formation early in the dormant period (Nelson 1978). In the current study, rapid tylose development in symptomatic *J. regia* trees occurred during the growing season when heartwood formation and ethylene production should be at their lowest. Since tyloses developed rapidly across all radial trunk depths, it is unlikely that apoplexy symptoms resulted simply from an acceleration of heartwood formation. If this were the case, sap flow would have ceased first at the innermost radial depth (i.e., closest to the heartwood) as tyloses formed at greater depth and then closer to the cambium as the season progressed.

Apoplexy disorder, as described in other crop trees, has been often attributable to pathogenic organisms (Kouyeas 1977, McDonald et al. 2009). For example, apoplexy of mature avocado trees growing in southern Spain experience sudden twig and branch dieback attributable to infection by *Neofusicoccum parvum* (Zea-Bonilla et al. 2007). Similarly, *Pseudomonas viridiflava* was identified as the main causal agent of foliage yellowing and sudden whole-tree dieback in nectarine trees (Scortichini and Morone 1997). Since apoplexy of other trees has been linked to plant pathogens, we conducted extensive pathogen screens on xylem sap extracts and leaf, petiole and stem tissues from asymptomatic and symptomatic trees in the study orchard (unpublished data). We found no conclusive evidence for the role of biotic organisms in symptom formation. However, some but not all apoplexy-afflicted trees tested positive for phytoplasmas.

Phytoplasmas cause leaf yellowing, stunting and branch dieback over several years and abnormal, excessive proliferation of axillary shoots resembling a broom on trunks and main stems in infected trees (Chen et al. 1992). The adventitious re-sprouting we documented did not resemble witches' broom and was not present prior to the apoplexy-induced leaf drop. Therefore, it seems unlikely that phytoplasmas are responsible for apoplexy. It is more likely that phytoplasma infection was secondary, occurring after initiation of apoplectic symptoms.

Drought-induced leaf yellowing and shedding has been linked to increased cavitation and embolism in the petioles of walnut leaves. Tyree et al. (1993) suggested that walnut hydraulic architecture is designed to sacrifice leaves during drought to protect more valuable woody parts from severe water stress. Here, we found that embolism was not significantly different between asymptomatic and symptomatic trees, and the reductions in stem K_s were irreversible (i.e., a high-pressure flush did not restore conductivity as would be the case for an embolized segment) due to tylose occlusions. Massive embolism throughout the entire crown prior to tylose formation is unlikely since significant cavitation and embolism formation does not occur in *J. regia* stems at Ψ_s above −2.0 MPa (Tyree et al. 1993; Cochard et al. 2002). Ψ_s measured in the current study only approached −1.8 MPa in yellowing leaves after the onset of symptoms. Stomatal closure prior to symptom formation also likely played a role in maintaining relatively high Ψ_s and avoiding cavitation despite the extensive formation of tyloses throughout the vasculature of apoplexy trees; similar stomatal closure under water stress has been previously reported in walnuts (Cochard et al. 2002).

Funding

This work was funded in part by USDA-ARS CRIS project 5306-22000-014-00 and the California Walnut Board.

Acknowledgments

Thanks to S. Biglieri of Biglieri Farms in Clements, CA for providing access to the orchard and for the use of ladders and equipment throughout the study; to K. Shackel, B. Lampinen, C. Brodersen and G.Gambetta for useful discussions about the datasets; to C. Manuck, F. Palladino, K. Pearsall and M. Macree for help with hydraulic conductivity, ethylene and sap flow measurements, pathogen sample preparation, tylose development and statistical analysis; to B. Martin for phytoplasma detection assays.

References

Abeles, F.B., P.W. Morgan and M.E. Saltveit Jr. 1992. Ethylene in plant biology. Academic Press, San Diego, CA, USA.

Aleemullah, M. and K.B. Walsh. 1996. Australian papaya dieback: evidence against the calcium deficiency hypothesis and observations on the significance of laticifer autofluorescence. Aust. J. Agric. Res. 47:371–385.

Arshad, M. and W.T. Frankenberger. 1991. Effects of soil properties and trace elements on ethylene production in soils. Soil Sci. Soc. Am. J. 151:377–386.

Bonsen, K.J.M. and L.J. Kučera. 1990. Vessel occlusions in plants: morphological, functional, and evolutionary aspects. IAWA Bull. 11:393–399.

Burgess, S.S.O., M.A. Adams, N.C. Turner, C.R. Beverly, C.K. Ong, A.A.H. Khan and T.M. Bleby. 2001. An improved heat pulse method to measure low and reverse rates of sap flow in woody plants. Tree Physiol. 21:589–598.

California Walnut Board. 2009. California Walnut History, Cultivation and Processing http://www.walnuts.org/walnuts101/history_cultivation_processing.php.

Chen, J., C.J. Chang and R.E. Jarret. 1992. DNA probes as molecular markers to monitor the seasonal occurrence of walnut witches'-broom mycoplasmalike organisms. Plant Dis. 76:1116–1119.

Cochard, H. and M.T. Tyree. 1990. Xylem dysfunction in Quercus: vessel sizes, tyloses, cavitation and seasonal changes in embolism. Tree Physiol. 6:393–407.

Cochard, H. L., X. Le Coll, Roux Le and T. Ameglio. 2002. Unraveling the effects of plant hudraulics on stomatal closure during water stress in walnut. Plant Physiol. 128:282–290.

Collins, B.R., J.L. Parke, B. Lachenbruch and E.M. Hansen. 2009. The effects of *Phytophthora ramorum* infection on the hydraulic conductivity and tylosis formation in tanoak sapwood. Can. J. For. Res. 39:1766–1776.

Davison, E.M. and F.S.C. Tay. 1985. The effect of waterlogging on seedlings of *Eucalyptus marginata*. New Phytol. 101:743–753.

Dimond, A.E. 1955. Pathogenesis in the wilt diseases. Annu. Rev. Plant Physiol. 6:329–350.

Dute, R.R., K.M. Duncan and B. Duke. 1999. Tyloses in abscission scars of loblolly pine. IAWA J. 20:67–74.

Eklund, L. 1990. Endogenous levels of oxygen, carbon dioxide and ethylene in stems of Norway spruce trees throughout a growth period. Trees Struct. Func. 4:150–154.

Eklund, L. 2000. Internal oxygen levels decrease during the growing season and with increasing stem height. Trees Struct. Func. 14:177–180.

Esau, K. 1977. Anatomy of seed plants. 2nd edition. Wiley, New York, NY, USA.

Fulton, A., R. Buchner, C. Little, C. Gilles, J. Grant, B. Lampinen, K. Shackel, L. Schwankl, T. Prichard and D. Rivers. 2002. Relationships between midday stem water potential, soil moisture measurement, and walnut shoot growth. Report to the California Walnut Board 135–143.

Grant, J.A., W.H. Olson and G.S. Sibbett. 2002. Apoplexy. Compendium of nut crop diseases in temperate zones. APS Press-The American Phytopathological Society, St Paul, MN, USA.

Hopkins, D.L. 1989. *Xylella fastidiosa*: xylem-limited bacterial pathogens of plants. Annu. Rev. Phytopathol. 27:271–290.

Hunt, P.G., R.B. Campbell, R.E. Sojka and J.E. Parsons. 1981. Flooding-induced soil and plant ethylene accumulation and water status response of field-grown tobacco. Plant Soil 59:427–439.

Jacobi, W.R. and W.L. MacDonald. 1980. Colonization of resistant and susceptible oaks by *Ceratocystis fagacearum*. Phytopathology 70:618–623.

Kallestad, J.C., T.W. Sammis, J.G. Mexal and V. Gutschick. 2007. The impact of prolonged flood-irrigation on leaf gas exchange in mature pecans in an orchard setting. Int. J. Plant Prod. 1:163–178.

Kouyeas, H. 1977. Stone fruit tree apoplexy caused by *Phytophthora* collar rot. EPPO Bull. 7:117–124.

Lampinen, B., R. Buchner, A. Fulton et al. 2004. Irrigation management in walnut using evapotranspiration, soil and plant based data. http://ucmanagedrought.ucdavis.edu/PDF/Lampinen%20et%20al%202004.pdf.

McDonald, V.T., S.C. Lynch and A. Eskalen. 2009. Identification and pathogenicity of *Botryosphaeria* species associated with avocado branch dieback and trunk canker in California. Phytopathology 99:S81.

McElrone, A.J., J.L. Sherald and I.N. Forseth. 2003. Interactive effects of water stress and xylem-limited bacterial infection on the water relations of a host vine. J. Exp. Bot. 54:419–430.

McElrone, A.J., S. Jackson and P. Habdas. 2008. Hydraulic disruption and passive migration by a bacterial pathogen in oak tree xylem. J. Exp. Bot. 59:2649–2657.

NASS. 2008. National Agricultural Statistics Service-US Department of Agriculture. California Walnut Objective Measurement Report 1–504 September 2008.

Nelson, N.D. 1978. Xylem ethylene, phenol-oxidizing enzymes, and nitrogen and heartwood formation in walnut and cherry. Can. J. Bot. 56:626–634.

Newbanks, D., A. Bosch and M.H. Zimmermann. 1983. Evidence for xylem dysfunction by embolism in Dutch Elm Disease. Phytopathology 73:1060–1063.

Parameswaran, N., H. Knigge and W. Liese. 1985. Electron microscopic demonstration of a suberised layer in the tylosis wall of beech and oak. IAWA Bull. 6:269–271.

Parke, J.L., E. Oh, S. Voelker, E.M. Hansen, G. Buckles and B. Lachenbruch. 2007. *Phytophthora ramorum* colonizes tanoak xylem and is associated with reduced stem water transport. Phytopathology 97:1558–1567.

Perez, A. and S. Pollack. 2005. Fruit and Tree Nuts Outlook/FTS-318/September 28, 2005. Economic Research Service, USDA, Washington, DC, USA.

Pérez-Donoso, A.G., L.C. Greve, J.H. Walton, K.A. Shackel and J. M. Labavitch. 2006. *Xylella fastidiosa* infection and ethylene exposure result in xylem and water movement disruption in grapevine shoots. Plant Physiol. 143:1024–1036.

Ranjani, K. and K.V. Krishnamurthy. 1988. Tyloses of the root wood of *Cassia fistula* L. Feddes Repert. 99:147–149.

Ross, N.W. 1976. Pests and diseases. Stanislaus Orchard Handbook. Bell Printing and Lithograph, Modesto, CA, USA, Pp14.5b–14.5c.

Ruzin, S.E. 1999. Plant microtechnique and microscopy. Oxford University Press, New York, NY, USA.

Scortichini, M. and C. Morone. 1997. Apoplexy of peach trees caused by *Psuedomonas viridiflava*. J. Phytopathol. 145:397–399.

Shain, L. and W.E. Hillis. 1973. Ethylene production in xylem of *Pinus radiata* in relation to heartwood formation. Can. J. Bot. 51:1331–1335.

Sperry, J.S., J.R. Donnelly and M.T. Tyree. 1988. A method for measuring hydraulic conductivity and embolism in xylem. Plant Cell Environ. 11:35–40.

Sun, Q., T.L. Rost and M.A. Matthews. 2006. Pruning-induced tylose development in stems of current-year shoots of *Vitis vinifera* (Vitaceae). Am. J. Bot. 93:1567–1576.

Sun, Q., T.L. Rost, M.S. Reid and M.A. Matthews. 2007. Ethylene and not embolism is required for wound-induced tylose development in stems of grapevines. Plant Physiol. 145:1629–1636.

Sun, Q., T.L. Rost and M.A. Matthews. 2008. Wound-induced vascular occlusions in *Vitis vinifera* (Vitaceae): tyloses in summer and gels in winter. Am. J. Bot. 95:1498–1505.

Taylor, A.M., B.L. Gartner and J.J. Morrell. 2002. Heartwood formation and natural durability—a review. Wood Fiber Sci. 34:587–611.

Tyree, M.T. and M.H. Zimmermann. 2002. Xylem structure and the ascent of sap. 2nd Edition. Springer, Berlin, Germany.

Tyree, M.T., H. Cochard, P. Cruziat, B. Sinclair and T. Ameglio. 1993. Drought-induced leaf shedding in walnut: evidence for vulnerability segmentation. Plant Cell Environ. 16:879–882.

VanderMolen, G.E., C.H. Beckman and E. Rodehorst. 1987. The ultrastructure of tylose formation in resistant banana following inoculation with *Fusarium oxysporum* f.sp. *cubense*. Physiol. Mol. Plant Pathol. 31:185–200.

van Doorn, W.G., H. Harkema and E. Otma. 1991. Is vascular blockage in stems of cut lilac flowers mediated by ethylene. Acta Hort. (ISHS) 298:177–182.

Voesenek, L.A.C.J., F.J.M. Harren, G.M. Bögemann, C.W.P.M. Blom and J. Reuss. 1990. Ethylene production and petiole growth in *Rumex* plants induced by soil waterlogging. Plant Physiol. 94:1071–1077.

Zea-Bonilla, T., M.A. González-Sánchez, P.M. Martín-Sánchez and R.M. Pérez-Jiménez. 2007. Avocado dieback caused by *Neofusicoccum parvum* in the Andalucia Region. Spain. Plant Dis. 91:1052.